Interactions defining the specificity between fungal xylanases and the xylanase-inhibiting protein XIP-I from wheat

Ruth FLATMAN*, W. Russell McLAUCHLAN*, Nathalie JUGE*†, Caroline FURNISS*, Jean-Guy BERRIN*†, Richard K. HUGHES*, Paloma MANZANARES‡, John E. LADBURY§, Ronan O'BRIEN§ and Gary WILLIAMSON*[1]

*Institute of Food Research, Colney Lane, Norwich NR4 7UA, U.K., †Institut Méditerranéen de Recherche en Nutrition, UMR INRA IIII, Faculté des Sciences et Techniques de Saint-Jérôme, Marseilles, F-13397 Cedex 20, France, ‡Instituto de Agroquímica y Tecnología de Alimentos, CSIC, P.O. Box 73, 46100 Burjassot, Valencia, Spain, and §University College London, Darwin Building, Gower Street, London WC1E 6BT, U.K.

We previously reported on the xylanase-inhibiting protein I (XIP-I) from wheat [McLauchlan, Garcia-Conesa, Williamson, Roza, Ravestein and Maat (1999), Biochem. J. **338**, 441–446]. In the present study, we show that XIP-I inhibits family-10 and -11 fungal xylanases. The K_i values for fungal xylanases ranged from 3.4 to 610 nM, but bacterial family-10 and -11 xylanases were not inhibited. Unlike many glycosidase inhibitors, XIP-I was not a slow-binding inhibitor of the *Aspergillus niger* xylanase. Isothermal titration calorimetry of the XIP-I–*A. niger* xylanase complex showed the formation of a stoichiometric (1:1) complex with a heat capacity change of $-1.38\ kJ \cdot mol^{-1} \cdot K^{-1}$, leading to a predicted buried surface area of approx. $2200 \pm 500\ Å^2$ at the complex interface. For this complex with *A. niger* xylanase (K_i = 320 nM at pH 5.5), titration curves indicated that an observable interaction occurred at pH 4–7, and this was consistent with the pH profile of inhibition of activity. In contrast, the stronger complex between *A. nidulans* xylanase and XIP-I (K_i = 9 nM) led to an observable interaction across the entire pH range tested (3–9). Using surface plasmon resonance, we show that the differences in the binding affinity of XIP-I for *A. niger* and *A. nidulans* xylanase are due to a 200-fold lower dissociation rate k_{off} for the latter, with only a small difference in association rate k_{on}.

Key words: plant inhibitor, protein–protein interaction.

INTRODUCTION

Proteinaceous inhibitors of invertase [1–3], limit dextrinase [4], polygalacturonase [5,6], pectinmethylesterase [7] and α-amylase [8,9] have all been identified in plants. The presence of proteinaceous xylanase inhibitors has also been reported in cereals [10–12]. Xylanases (endo-β-1,4-xylanases) hydrolyse the β-1,4-xylan linkages in the xylan component of plant cell walls. Based on sequence and structural homology, they have been classified into family-10 and -11 (EC 3.2.1.8) glycoside hydrolases [13,14]. Family-10 xylanases (> 30 kDa) are generally larger than family-11 xylanases (approx. 20 kDa) with an $(\alpha/\beta)_8$ barrel fold, whereas family-11 xylanases consist of a single domain composed predominantly of β-strands [15]. Xylanase-inhibiting protein I (XIP-I) has been purified from wheat flour and partially characterized [16]. It is a glycosylated, monomeric basic protein with a molecular mass of 29 kDa, and a pI of 8.7–8.9. XIP-I has been shown to inhibit two family-11 xylanases, from *Trichoderma viride* and *Aspergillus niger* respectively, and the inhibition was competitive for the *A. niger* enzyme. Another proteinaceous xylanase inhibitor from wheat, *Triticum aestivum* xylanase inhibitor (TAXI), has also been described [12]. It is in fact a mixture of two endoxylanase inhibitors TAXI I and TAXI II, which differ from each other in pI and endoxylanase specificity, but show structural homology [17]. Based on the limited information from protein sequencing [17], there is no sequence homology between XIP-I and TAXI. We present for the first time a detailed study of XIP-I inhibition to determine its specificity, pH dependence, mode of action and the thermodynamics of the interaction. This is the first mechanistic study of any xylanase inhibitor.

EXPERIMENTAL

Materials

Medium viscosity wheat arabinoxylan was from Megazyme (County Wicklow, Ireland). *Trichoderma viride* xylanase, two xylanases from *Trichoderma longibrachiatum* and a rumen microorganism xylanase (M1, M2, M3 and M6 respectively) were from Megazyme. *Penicillium funiculosum* xylanase (native and *Escherichia coli* recombinant forms) was from our in-house collection, *A. oryzae* xylanase was from M. Tenkanen (VTT, Finland), *A. aculeatus* and *Bacillus subtilis* xylanases were from J. Delcour (Laboratory of Food Chemistry, Katholieke Universiteit Leuven, Belgium), *Fibrobacter succinogenes* xylanase domains A and B were from A. Clarke (University of Guelph, Canada), *B. agaradhaerens* xylanase was from G. Davies (University of York, U.K.), *Pseudomonas fluorescens* xylanase was from H. Gilbert (University of Newcastle, U.K.) and the recombinant *E. coli* clone producing *Bacillus* sp. xylanase was from F. J. Pastor (University of Barcelona, Spain).

Purification of xylanase inhibitor from wheat flour

The xylanase inhibitor was purified from 2 kg of wheat flour (*Triticum aestivum* var. Soisson) as described previously [16].

Abbreviations used: IEF, isoelectric focusing; ITC, isothermal titration calorimetry; MALDI-TOF, Matrix-assisted laser-desorption ionization time-of-flight; SPR, surface plasmon resonance; TAXI, *Triticum aestivum* xylanase inhibitor; XIP-I, xylanase-inhibiting protein I.

[1] To whom correspondence should be addressed, at the Nestlé Research Center, P.O. Box 44, CH-1000, Lausanne 26, Switzerland (e-mail gary.williamson@rdls.nestle.com).

Identification of XIP-I protein peak

The final step in the purification procedure of the xylanase inhibitor yielded two protein peaks as expected showing almost identical specific inhibitory effects and physical properties [16]. Initial characterization of the inhibitor was performed using the first protein peak ('peak 1'). In order to determine the exact nature of the two peaks, flour extracts were partially purified by cation-exchange and ammonium sulphate precipitations, as described previously [16], and they were treated as follows. After centrifugation, the pellet was dissolved in distilled water (10 ml), dialysed against 20 mM Tris/HCl (pH 7.0), and divided into three 2 ml aliquots. Each sample was then mixed either with the Tris/HCl buffer on its own or with the buffer supplemented with the inhibitor (0.5 mg) from peaks 1 and 2 respectively. The mixtures were then loaded on to Mono S columns, which were previously equilibrated with the same buffer, and proteins were eluted for 60 min with a gradient of 0–0.3 M NaCl in equilibration buffer. The fractions were then assayed for inhibitory activity. With the unsupplemented flour extract, only one peak of inhibitory activity was detected corresponding to 'inhibitor peak 2', which suggested that XIP-I corresponded to peak 2 and that the two peaks at the end of the purification were due to minor modification during the purification process. When the flour sample was supplemented with the inhibitor from peak 1, two peaks of inhibitory activity were detected, as expected. However, the third sample, which was supplemented with inhibitor peak 2, also produced two peaks of inhibition, although peak 1 was smaller than peak 2; this result suggested that storage of peak 2 led to a modification of the protein, which gave rise to a small amount of peak 1.

In order to confirm the effect of storage conditions, the individual inhibitors (0.2 mg) from peaks 1 and 2, stored at 4 °C for 4 weeks, were applied on to a Mono S column. When inhibitor peak 1 alone was applied to the column, one peak of inhibition was produced, but when inhibitor peak 2 was applied to the column two peaks of inhibition could be detected. Taken together, these results showed that inhibitor peak 2 is the native form of the inhibitor. In contrast, 'inhibitor peak 1' is a modified form produced both during the purification process and on storage, although the properties are apparently not modified. As a result of this, all experiments in the present study were conducted on inhibitor peak 2, which is hereafter referred to as XIP-I.

Matrix-assisted laser-desorption ionization time-of-flight (MALDI-TOF)-MS

XIP-I was analysed using a MALDI-TOF-MS (Bruker Reflex III; Bruker Daltonik GmbH, Bremen, Germany) mass spectrometer, equipped with 337 nm N_2 laser. The sample (10 μM) was mixed with an equal volume of matrix solution (10 mg/ml of sinapinic acid in 50 % acetonitrile, 0.1 % trifluoroacetic acid), and 0.5 μl of this mixture was applied to the sample well and dried at 22 °C. The sample well was then washed twice with water (4 μl), wicked off with tissue after approx. 20 s and dried again. The matrix solution (0.5 μl) was then applied on top of each sample, and the samples were dried and analysed by MALDI-TOF. Spectra were accumulated from 770 laser shots with 5 ns intervals at 43 % laser alternation. The molecular mass of XIP-I was determined by this method to be 30657 kDa.

Isolation of recombinant proteins

Large-scale expression of *A. niger* xylanase in *Pichia pastoris* was achieved as described previously [18]. The supernatant was concentrated by using a 200 ml stirred ultrafiltration cell (model 202; Amicon, Stonehouse, Gloucestershire, U.K.) and a PM10 ultrafiltration membrane (Millipore, Watford, Herts., U.K.), and the protein was purified to homogeneity using the procedure described previously [18].

A. nidulans xylanase was purified from an *A. nidulans* multicopy transformant [19] as follows. The culture filtrate was adjusted to pH 5.5 with 0.1 M HCl and then diluted twice. The secreted proteins were adsorbed batchwise on DEAE-Sephadex A-50. After overnight stirring, the resin was transferred on to a glass column and the adsorbed proteins were pulse-eluted with 10 mM sodium phosphate buffer (pH 5.5) containing 1 M NaCl. Fractions containing xylanase activity were loaded on to a Superose 12 column pre-equilibrated with 20 mM sodium acetate buffer (pH 5.5) containing 100 mM NaCl. Active fractions were pooled and desalted and used throughout the study.

Recombinant *E. coli* producing *Bacillus* sp. xylanase was grown in Luria–Bertani broth supplemented with ampicillin (50 μg/ml) at 37 °C overnight. The culture was centrifuged at 10000 ***g*** for 20 min at 4 °C, and the cells were resuspended in 5 ml of McIlvaine buffer (pH 5.5) and lysed by sonication (Sonopuls HD 2070; Bandelin, Berlin, Germany). The cell debris was removed after centrifugation at 6000 ***g*** for 20 min at 4 °C, and the supernatant was used for xylanase activity assay.

Activity assays

For the measurement of protein concentrations, either the Coomassie Brilliant Blue method of Bradford [20] was used with BSA (Perbio Science Ltd, Cheshire, U.K.) as the standard, or the reported molar absorption coefficients ϵ, where available, were used. Using primary structure analysis (http://www.expasy.ch/), the ϵ_{280} values were determined to be 50210, 57180, 68050, 56470, 41960, 62870 and 59030 $M^{-1} \cdot cm^{-1}$ for the xylanases from *A. niger* (1UKR), *P. funiculosum* (AJ278385.1), *A. nidulans* (Z49894), *B. agaradhaerens* (1QH6), *F. succinogenes* A and B domains (P35811) and *Ps. fluorescens* (X15429) respectively. The codes in parentheses are the National Center for Biotechnology Information accession nos. or Protein Data Bank codes.

Xylanase activity was measured using the dinitrosalicylic acid assay [21]. Enzyme samples (10 μl) were added to wheat arabinoxylan (90 μl) solubilized in McIlvaine buffer (0.1 M citric acid/0.2 M Na_2HPO_4; pH 5.5) and incubated at 30 °C for different time periods (4–35 min). The relationship between time or enzyme concentration and activity was checked to ensure linearity of the reaction. The enzyme preparations were checked for purity on SDS/PAGE and most gave a single band (results not shown). When extra bands were observed, the sample was spiked with *A. niger* xylanase and XIP-I to ensure that the contaminant proteins did not affect the interaction. The reaction was terminated by the addition of dinitrosalicylic acid reagent (150 μl), and the samples were boiled for 5 min and then cooled to 22 °C. After centrifugation at 13000 ***g*** for 5 min, the supernatant (200 μl) was transferred on to a microtitre plate and ϵ_{550} was measured relative to a xylose standard curve (0–180 μg/ml). Units are expressed as μmol of xylose produced/min. To determine whether XIP-I was a slow-binding inhibitor, the enzyme and the inhibitor were mixed for different incubation time periods from 0 to 20 min, at 1 or 2 min intervals, before addition of the substrate to initiate the reaction.

The kinetic constants for xylanase activity were calculated using weighted non-linear least-squares regression analysis with the Grafit software program (Biosoft, Cambridge, U.K.). Inhibition was detected by adding increasing molar equivalents of XIP-I to the enzyme solution up to a maximum molar ratio of

30:1. The IC_{50} value was determined at the K_m of the enzyme and corresponded to the molar concentration of XIP-I required to inhibit xylanase activity by 50 %. The K_i value was determined at different concentrations of substrate (1.5–18 mg/ml) in the presence of various amounts of XIP-I. The Grafit software program was used to calculate the K_m and V_{max} for each inhibitor concentration. We assume that $K_i \approx K_d$, since the inhibition is competitive. In the present study, we use K_i and K_d to denote kinetic and thermodynamic measurements.

To determine the optimum pH for binding, the xylanase activity assay was performed as described above, using wheat arabinoxylan (1 %, w/v) at pH 3.4–6.5. *A. niger* xylanase (0.17 μM) and XIP-I (0.65 μM) were added to the assay and longer incubation time periods were used to compensate for the very low enzyme activity at higher pH values. All incubation time periods were first checked to ensure linearity.

Surface plasmon resonance (SPR)

BIAcore X system, HBS buffer [10 mM Hepes (pH 7.4)/0.15 M NaCl/3.4 mM of EDTA/0.005 % of surfactant P20], CM5 sensor chips and amine coupling kit were from BIAcore AB (Uppsala, Sweden). XIP-I (1 μM) in 10 mM sodium acetate buffer (pH 5.5) was immobilized by the amine coupling method of Johnsson et al. [22] at a flow rate of 10 μl/min, using HBS buffer as running buffer. Briefly, equal volumes of *N*-hydroxysuccinimide (NHS, 0.06 M in water) and *N*-ethyl-*N*′-(3-diethylaminopropyl)carbodiimide (0.2 M in water) were mixed and injected on to a CM5 sensor chip to activate the carboxymethylated dextran surface. The volume used was adjusted to achieve immobilization levels of XIP-I giving 150–2000 resonance units (RU); 1 RU is defined as 1 pg of bound protein/mm². After injection of XIP-I (40 μl), the residual NHS esters were deactivated by the injection of 25 μl of ethanolamine (1 M, pH 8.5). Flow cell 2 was used to immobilize XIP-I, and control flow cell 1 was treated identically but without inhibitor.

For *A. niger* xylanase, increasing concentrations of enzyme (80 μl) ranging from 0.3 to 13 μM in 10 mM sodium acetate (pH 5.5) were injected at a flow rate of 30 μl/min, using 10 mM sodium acetate (pH 5.5) as running buffer. For *A. nidulans* xylanase, four separate chips were used, as adequate regeneration could not be achieved. The enzyme (80 μl) was injected at a concentration of 600 nM on to three separate chips at a flow rate of 30 μl/min and a further 40 μl of the sample (450 nM) was injected on to a fourth chip at a flow rate of 10 μl/min. The sensorgram shows the change in resonance signal as a function of time [23].

Isoelectric focusing (IEF) titration curves

Titration curves of either the xylanases alone or the xylanases in combination with XIP-I were produced using the Phast system (Amersham Pharmacia Biotech, Uppsala, Sweden). IEF 3–9 gels (Amersham Pharmacia Biotech) were used according to the manufacturer's instructions. Following a prefocusing step (2000 V, 150 V · h), samples were applied across the middle of the gel and focused for 60 V · h at 1000 V. For staining, the gels were fixed for 20 min in trichloroacetic acid (20 %, w/v), rinsed in phosphoric acid solution (3 %), incubated for 10 min with SERVA Violet 17 stain (0.2 % SERVA Violet/20 % phosphoric acid, 1:1; SERVA Electrophoresis GmbH, Heidelberg, Germany) and washed three times (10 min) using phosphoric acid (3 %). For silver staining, the PhastGel™ silver kit was used according to the manufacturer's instructions (Amersham Pharmacia Biotech).

Isothermal titration calorimetry (ITC)

Enthalpy values for the interaction of the *A. niger* xylanase with XIP-I were determined at the temperatures 10, 17.5, 25 and 33 °C using a VP isothermal titration calorimeter (Microcal, Milton Keynes, U.K.). The enzyme (100 μM) and the inhibitor (10 μM) were dialysed extensively against McIlvaine buffer (pH 5.5). During a titration, the inhibitor (2.3 ml) placed in the reference cell was injected with 16 successive aliquots of enzyme (15 μl) at 5 min intervals for approx. 80 min. The binding data were corrected for the heat of dilution of both proteins. Integrated heat effects were analysed by non-linear regression using a single-site binding model with Origin software (Microcal), yielding independent values for K_d and $\Delta H°$ [24]. Enthalpy changes at the four temperatures were plotted against temperature; the slope of the line gave the change in heat capacity [25,26]. Changes in negative heat capacity have been linked to the removal of non-polar surface area from water in protein processes [27], and an equation linking the removal of polar and non-polar surface area has been formulated [28], which was used to predict the surface area that becomes buried on the association of XIP-I and *A. niger* xylanase.

RESULTS

Further characterization of the interaction between *A. niger* xylanase and XIP-I

We have previously shown that XIP-I inhibited, reversibly and in a competitive manner, a family-11 xylanase from *A. niger* [16]. Further characterization of the inhibition type was assessed by preincubation of *A. niger* xylanase with XIP-I before the activity assay. None of the extra preincubation steps, of 0, 1, 2, 3, 5, 7, 9, 10, 11, 12, 14, 15, 17, 18 and 20 min, led to an increase in the observed reaction rate (results not shown). This criterion has been used in a previous study [29] to define a 'slow-binding' inhibitor. It was evident from the above results that XIP-I is not a slow-binding inhibitor.

The effect of pH on the binding of XIP-I to *A. niger* xylanase was measured over the pH range 3.5–6.5. The percentage of inhibition appeared to be inversely related to the enzyme activity (Figure 1). Optimal activity of *A. niger* xylanase was at pH 3.5 with a gradual decrease above the pH optimum, 14 % remaining at pH 6.5. Inhibition was not detected under the experimental

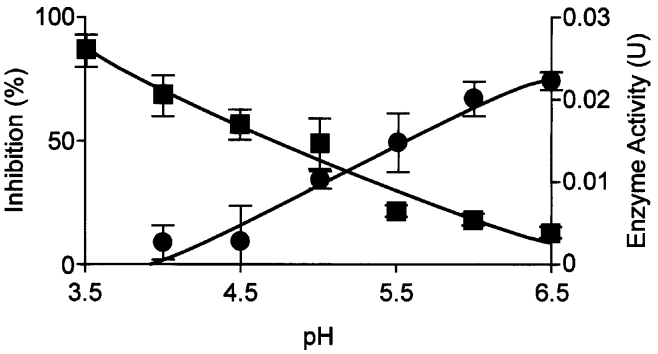

Figure 1 Effect of pH on inhibition of *A. niger* xylanase by XIP-I

■, Uninhibited enzyme activity; ●, inhibition percentage. Error bars represent ±S.D. ($n = 4$).

Table 1 Thermodynamic parameters for the interaction of XIP-I with *A. niger* xylanase

Temperature (K)	Stoichiometry	Affinity, K_d (nM)	Enthalpy change, ΔH (kJ/mol)	Entropy change ΔS (kJ · mol^{-1} · K^{-1})	Free energy change, ΔG (kJ/mol)
283	0.915 ± 0.010	3.52 ± 5.27*	−24.86 ± 0.63	0.074	−45.8
290.5	0.935 ± 0.005	13.3 ± 3.82	−34.79 ± 0.42	0.031	−43.8
298	0.901 ± 0.004	41.5 ± 6.15	−48.49 ± 0.47	−0.021	−42.1
306	0.885 ± 0.005	35.0 ± 6.52	−55.76 ± 0.71	−0.039	−43.7

* The heats measured were low, and the error reflects this.

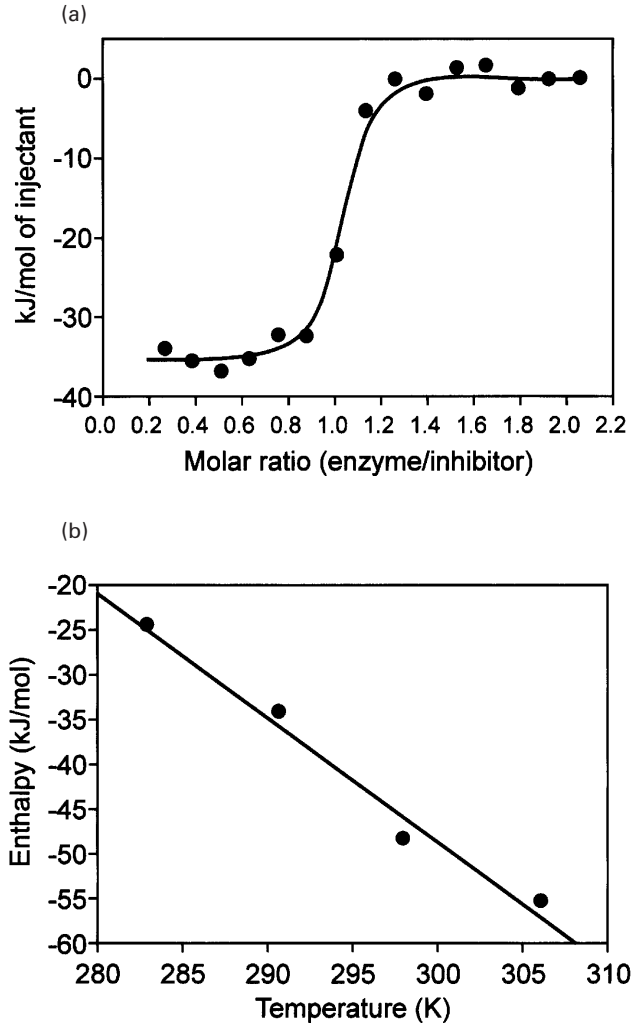

Figure 2 Thermodynamics of the interaction using ITC

(**a**) Enthalpy change on binding of *A. niger* xylanase to XIP-I. Data are shown at 290.5 K as a function of molar ratio, with integrated data after correction for heat of ligand dilution, presented as heat exchange (kJ/mol of injectant), versus the molar ratio of enzyme to inhibitor. The solid line shows the best fit obtained by least-squares regression using a one-site model. This analysis gave a determined stoichiometric value of 0.94. (**b**) Temperature dependence of the enthalpy change for *A. niger* xylanase binding to XIP-I. The linear dependence of enthalpy versus temperature yields a heat capacity change ΔC_p of -1.38 kJ · mol^{-1} · K^{-1} (± 0.122) ($R^2 = 0.98$).

conditions at pH 3.5, was negligible at pH 4 and gradually increased over the pH range 4.5–6.5; this result demonstrated the involvement of electrostatic charges in the interaction.

ITC showed a stoichiometry approximating to unity in all the experiments (Table 1). The interaction was enthalpy-driven at 290.5 K (Figure 2a). The temperature dependence of the enthalpy gave a change in heat capacity of -1.38 kJ · mol^{-1} · K^{-1} (Figure 2b). Based on the empirically derived correlation between ΔC_p and removal of surface area from exposure to bulk solvent, and, assuming that the ratio of $\Delta A_p/\Delta A_{np} = 0.59$, we can predict a value for the area of the binding site [28]. Using the equation

$$\Delta C_p = (1.34 \pm 0.17)\Delta A_{np} - (0.59 \pm 0.17)\Delta A_p \text{ J} \cdot \text{mol}^{-1} \cdot \text{K}^{-1}$$

the overall surface area buried on binding was calculated to be 2200 ± 500 Å^2. This was the result of a change in the surface areas of the polar group (ΔA_p) and non-polar group (ΔA_{np}) of 830 ± 230 and 1400 ± 310 Å^2 respectively. The total calculated surface areas for the individual proteins *A. niger* xylanase and XIP-I were 7623 and 11715 Å^2 respectively (Roussel, A., personal communication), indicating that approx. 15 and 10% respectively of the surface area of each protein is buried on formation of the complex.

Specificity of XIP-I towards xylanases

The specificity of XIP-I towards xylanases was assessed using a range of fungal and bacterial xylanases from families 10 and 11. XIP-I could inhibit fungal xylanases but no bacterial xylanase was inhibited up to a molar ratio of 30:1 (Table 2). Interestingly, all the fungal xylanases tested were inhibited apart from the family-10 *A. aculeatus* xylanase (Table 2). This inhibition of fungal xylanases was not due to the binding of XIP-I to glycosylation on the fungal enzymes, since both the native and *E. coli*-expressed recombinant forms of *P. funiculosum* xylanase were inhibited to the same extent (Furniss, C., unpublished work). The K_i values for fungal xylanases ranged from 3.4 to 610 nM for *P. funiculosum* and *Trichoderma viride* xylanases respectively. XIP-I did not show a preference for family-10 or -11 xylanases, since the two tightly binding complexes were formed with the *P. funiculosum* and *A. nidulans* xylanases, belonging to families 11 and 10 respectively. As previously found for *A. niger* xylanase [16], the inhibition was competitive for all the enzymes tested. As an example, the kinetics of the inhibition is reported below for a family-10 fungal xylanase from *A. nidulans*. An 18 nM concentration of XIP-I was required to inhibit 31 nM of *A. nidulans* xylanase by 50%, i.e. a molar ratio of enzyme to inhibitor of 1.7:1 (Figure 3). Double-reciprocal plots for the interaction of XIP-I with the *A. nidulans* xylanase are shown in Figure 4(a). The convergence of the lines at the *y*-axis shows that increasing the concentration of XIP-I did not change V_{max}, but increased K_m. This indicates that the inhibition was competitive. A secondary plot of slopes against XIP-I concentration (Figure 4b) gave an inhibition constant K_i of 9 nM at pH 5.5.

Table 2 Specificity and kinetics of inhibition

n.d., not determined; n.a., not applicable.

Source	Family	Is enzyme inhibited at its K_m?*	Molar ratio of E:I†	K_i (nM)	Inhibition type
Fungal					
A. niger	11	Yes	1:3.8	317	Competitive
Trichoderma viride	11	Yes	1:63	610	Competitive
T. longibrachiatum M2	11	Yes‡	N/D	N/D	Competitive
T. longibrachiatum M3	11	Yes	1:5.3	20	Competitive
P. funiculosum§	11	Yes	1:1	3.4	Competitive
A. nidulans	10	Yes	1:0.6	9	Competitive
A. oryzae	10	Yes	1:1.5	17	Competitive
A. aculeatus	10	No	n.a.	n.a.	n.a.
Bacterial					
B. agaradhaerens	11	No	n.a.	n.a.	n.a.
F. succinogens (A)	11	No	n.a.	n.a.	n.a.
F. succinogens (B)	11	No	n.a.	n.a.	n.a.
B. subtilis	11	No	n.a.	n.a.	n.a.
Ps. fluorescens	10	No	n.a.	n.a.	n.a.
Rumen micro-organism	11	No	n.a.	n.a.	n.a.
Bacillus sp.	10	No	n.a.	n.a.	n.a.

* Where no inhibition is detected, a 30:1 molar ratio of XIP-I to enzyme has been used, with 10% of inhibition being the limit of detection.
† The molar ratio that gives 50% inhibition.
‡ The K_m value was not determined owing to the limited solubility of the substrate: inhibition was observed at a substrate concentration of 5 mg/ml of wheat arabinoxylan.
§ Furniss, C., unpublished work.

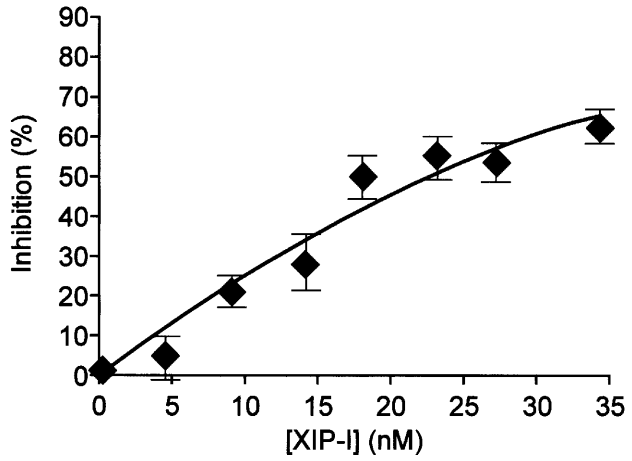

Figure 3 Inhibition curve of *A. nidulans* xylanase (31 nM) by increasing amounts of XIP-I

XIP-I (18 nM) inhibited the enzyme by 50%. Error bars represent ±S.D. ($n = 4$).

Interaction of XIP-I with family-10 and -11 fungal xylanases

The relative affinity and pH dependence of the interaction of XIP-I with *A. niger*, *A. nidulans* and *Pseudomonas fluorescens* xylanases were further studied using titration curves (Figures 5a–5c). The pI values of *A. niger* and *A. nidulans* xylanases are 3.5 [18] and 3.4 [19] respectively, whereas the pI value of XIP-I ranges from 8.7 to 8.9 [16]. Both *A. niger* xylanase ($K_i = 317$ nM) and *A. nidulans* xylanase ($K_i = 9$ nM) formed a complex on the IEF titration gel (Figures 5a and 5b). The complex was observed over a pH range of approx. 4–7 with *A. niger* xylanase (Figure 5a), but across the entire pH range (3–9; the range covered on the gel) in the case of *A. nidulans* xylanase (Figure 5b). The higher affinity of XIP-I for *A. nidulans* xylanase is further indicated by the fact that all the concentration-limited components form the complex (Figure 5b). Traces of *A. nidulans* xylanase can be seen on the gel when the enzyme to inhibitor molar ratio is 3:1 [Figure 5b(ii)], but they disappear when the amount of XIP-I is increased to a 3:2 molar ratio of enzyme to inhibitor, and some traces of XIP-I appear [Figure 5b(iii)]. By contrast, this result was not observed with *A. niger* xylanase. Owing to the weaker interaction, free enzyme was still observed at both high and low pH, even at a 1:6 molar ratio of enzyme to inhibitor (results not shown). No complex was formed when *Ps. fluorescens* xylanase and XIP-I were run on these gels (Figure 5c), in agreement with results from the activity assays.

We have shown the clear difference in affinity of XIP-I towards *A. niger* and *A. nidulans* xylanases from activity assays and titration curves. SPR allows direct visualization of molecular interactions in real time and hence of on and off rates, and was used to compare further the interaction of XIP-I with these two enzymes. XIP-I was immobilized on the dextran surface of a chip, and the association/dissociation rate constants were calculated for the interaction of XIP-I with the xylanases. The overlaid sensorgrams for the interaction of XIP-I with *A. niger* xylanase are shown in Figure 6. For each concentration, the increase in RU from the initial baseline represents the binding of the xylanase to the surface-bound XIP-I. The plateau line represents the steady-state/equilibrium phase of the xylanase–XIP-I interaction, whereas the decrease in RU from the plateau represents the dissociation phase. Kinetic parameters, equilibrium constants and the enthalpy change for the interactions are shown in Table 2. *A. niger* xylanase exhibited a fast off rate, which is in agreement with the activity assay; this is again not consistent with the inhibitor following a slow-binding mechanism [30]. The enzymes exhibited similar on rates, but there was a 200-fold difference in off rates between *A. niger* xylanase and *A. nidulans* xylanase. Since $K_d \sim K_i = k_{off}/k_{on}$, the difference in off rates could account substantially for the 500-fold differences in the K_i values (Table 3).

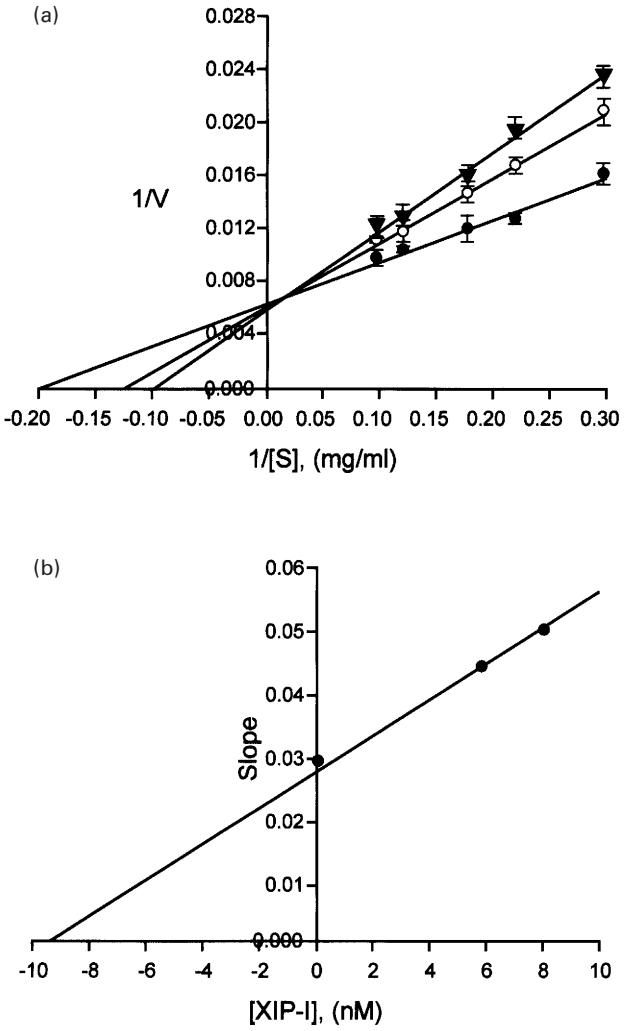

Figure 4 Kinetics of the interaction by measuring inhibition of xylanase activity

(**a**) A double-reciprocal plot for xylanase activity. ●, In the presence of inhibitor; ○, in the presence of 5.4 nM of XIP-I; ▼, in the presence of 8.0 nM of XIP-I. Error bars represent ± S.D. ($n = 4$). (**b**) Secondary plot of slopes (from the double-reciprocal plot) against inhibitor concentration to give K_i. Analysis was performed by non-linear regression; the data are shown for illustrative purposes only.

DISCUSSION

XIP-I inhibition: mechanism, type and mode of action

The inhibition mechanism of XIP-I against family-10 and -11 fungal xylanases has been studied in detail. The inhibition is competitive, suggesting that the inhibitor protein binds at, or close to, the active site, thus preventing access of the substrate to the active site. The magnitude of inhibition of the fungal xylanases by XIP-I varies 200-fold, based on K_i values from activity assays, depending on the xylanase tested. Slow binding, or slow onset of inhibition, is a widespread phenomenon among glycosidase inhibitors [31], where the inhibition process is relatively slow, occurring over a period of minutes and not at diffusion-controlled rates. This type of inhibition has been widely reported not only for substrate–analogue types of inhibitors, but also for protein inhibitors of glycosyl hydrolases such as αAI [9,29,32] and the invertase inhibitor from maize [1]. However, XIP-I does not appear to follow such an inhibition process, as observed for the *A. niger* xylanase using both activity assays and SPR. The enzyme exhibits a fast off rate as shown by SPR, whereas a slow off rate is characteristic of slow-binding inhibitors [30]. Kinetic analysis using SPR indicated that the difference in off rates largely accounted for the differences in binding strengths of the enzyme–inhibitor complexes.

The inhibition of *A. niger* by XIP-I is pH dependent over the pH range 4–7, as determined by activity assays and titration curves. This illustrates the importance of electrostatic interactions in the strength of the interaction. Such pH dependence was also observed in the case of barley α-amylase/subtilisin inhibitor [33], although in a broader range. However, the complex of *A. nidulans* seemed to be pH independent over the pH range 3–9, indicating strong binding. The large difference in K_i (approx. K_d) values was further characterized by using SPR, and this revealed a striking difference in the on and off rates. Although the on rate for the XIP-I–*A. nidulans* interaction was only 2-fold faster than the on rate for the XIP-I–*A. niger* interaction, the off rate was 200-fold slower and therefore accounted for the large differences in K_i values reported for these enzymes. The corresponding ΔG values for the interaction of XIP-I with *A. niger* xylanase and *A. nidulans* xylanase were -29.9 and -45.3 kJ · mol^{-1} respectively. The difference in K_i values between the two enzymes was greater than that found from activity assays; this probably reflects the 5° lower temperature, lower ionic strength buffer and more restricted conformation of XIP-I, in SPR determinations. The K_i values were comparable for XIP-I–*A. nidulans*, but the K_i was somewhat higher for XIP-I–*A. niger* using SPR, and lower using ITC.

ITC showed a stoichiometry approximating to unity in the binding of XIP-I on to *A. niger* xylanase. It also allowed the calculation of the surface area buried at the complex interface. Lo Conte et al. [34] collected the interface areas of a number of enzyme–inhibitor complexes and the average value was found to be 2030 Å^2 (S.D. = 630). Comparing the three-dimensional structures of free enzyme and inhibitor proteins with their respective complexes, it was observed that when a large interfacial surface area (> 2000 Å^2) was buried, a kinetically significant conformational change was often involved in complex formation. Such a structural change has been shown to occur at the active site of the porcine pancreatic α-amylase after the binding of the protein inhibitor from *Phaseolus vulgaris*, leading to 3080 Å^2 buried at the interface [35]. The interface area of the XIP-I–*A. niger* complex was predicted to be 2200 Å^2 (± 500). This means that there is a significant release of water at the interface, which contributes to the positive entropy changes observed at 283 and 290.5 K. However, at all four temperatures used in this experiment, binding was enthalpy-driven. A large change in surface area during the passage from the free protein to the complex may also result from a conformational change. This conformational change has often been reported as a feature of a slow-binding mechanism, involving two steps: either an initial fast-binding step, followed by a slow reversible transformation of EI to another entity, or an initial slow inter-conversion of the enzyme E into another form, which then binds the inhibitor in a fast step. However, the sensorgram obtained by SPR on the *A. niger* xylanase does not exhibit the typical shape characteristic of a conformational change. This is also in agreement with the activity assays showing that XIP-I is not a slow-binding inhibitor.

XIP-I specificity: comparison with other plant protein inhibitors of glycoside hydrolases

Further characterization of XIP-I revealed that it is a competitive inhibitor of fungal xylanases, but none of the bacterial xylanases

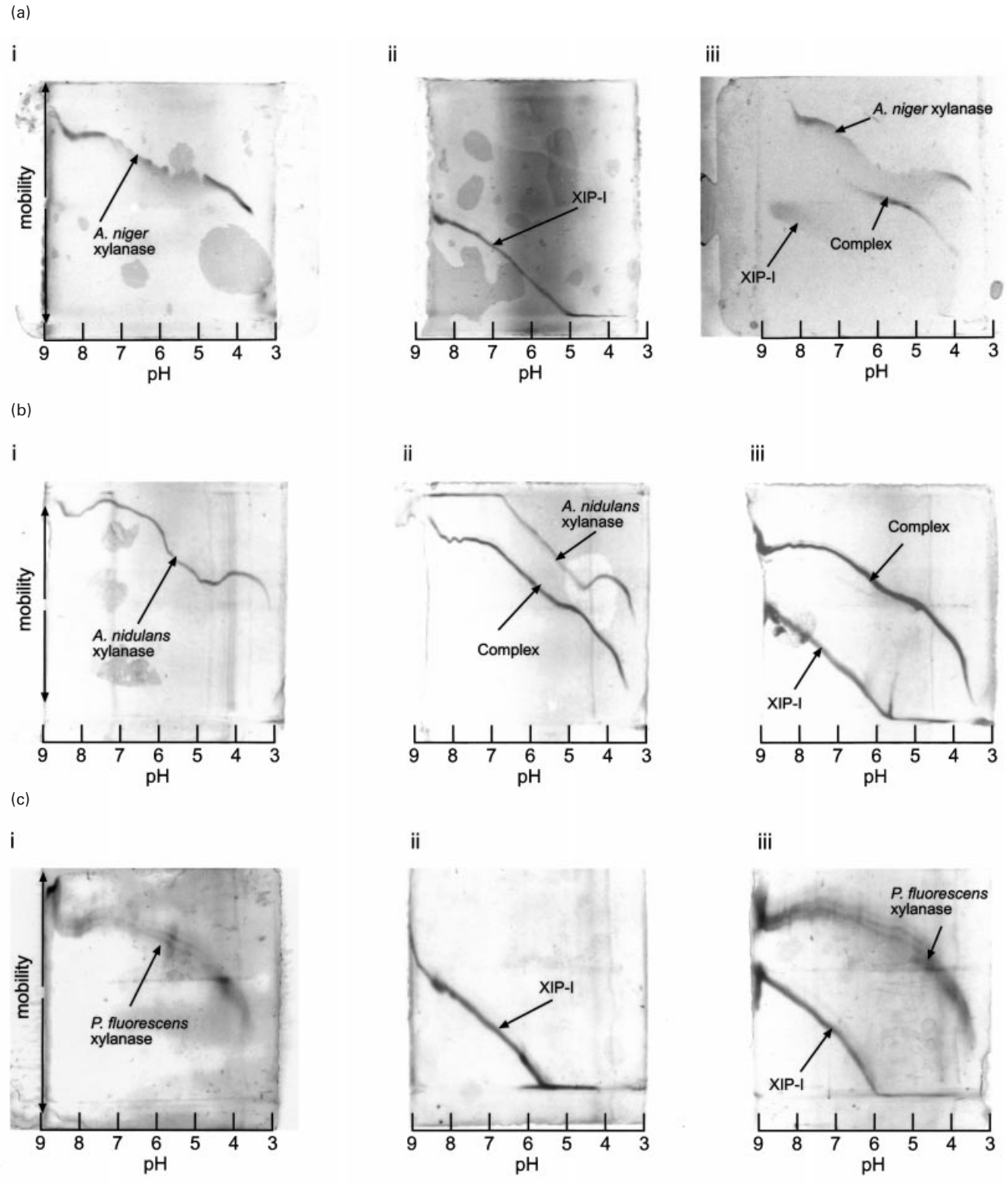

Figure 5 Titration curves, obtained by IEF, showing the interaction between XIP-I and xylanases

(**a**) Titration curves showing the interaction between *A. niger* xylanase and XIP-I. (i) *A. niger* xylanase (4 μg); (ii) XIP-I (4 μg); (iii) a mixture containing *A. niger* xylanase (5 μg) and XIP-I (4 μg). (**b**) Titration curves showing the interaction between *A. nidulans* xylanase and XIP-I. (i) *A. nidulans* xylanase (250 ng); (ii) a mixture of *A. nidulans* xylanase (250 ng) and XIP-I (70 ng); (iii) a mixture of *A. nidulans* xylanase (250 ng) and XIP-I (140 ng). (**c**) Titration curves showing the interaction between *Ps. fluorescens* xylanase and XIP-I. (i) *Ps. fluorescens* xylanase (520 ng); (ii) XIP-1 (200 ng); (iii) a mixture of *Ps. fluorescens* xylanase (520 ng) and XIP-I (200 ng).

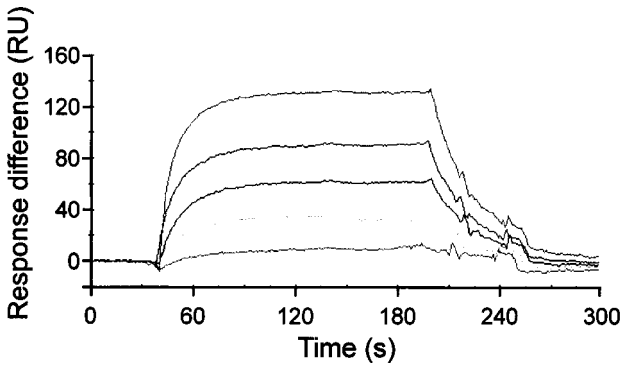

Figure 6 SPR sensorgrams showing the interaction between XIP-I and *A. niger* xylanase

Curves (from bottom to top) show the concentrations of *A. niger* xylanase: 0.32, 1.3, 2.6, 5.4 and 13 μM.

Table 3 SPR analysis of the interaction between XIP-I and the xylanases from *A. niger* and *A. nidulans*

Sensorgrams were analysed using 1:1 Langmuir binding. The K_d values were calculated as off rate/on rate (k_{off}/k_{on}). The free energy of the complex formation was calculated from the equation $\Delta G = RT \ln K_d$. Values are means $\pm$ S.D., $n = 3$ (*A. niger*) or 4 (*A. nidulans*).

Enzyme	On rate ($M^{-1} \cdot s^{-1}$)	Off rate (s^{-1})	K_d (μM)	ΔG (kJ/mol)
A. niger	6530 $\pm$ 120	0.0371 $\pm$ 0.0004	5.68	-29.9
A. nidulans	15000 $\pm$ 390	0.000172 $\pm$ 0.000002	0.0115	-45.3

tested was inhibited. The strict preference for fungal xylanases is not due to potential glycosylation of the enzyme. This strict specificity, along with other biochemical characteristics, distinguishes XIP-I from the other xylanase inhibitors TAXI I and TAXI II recently isolated from wheat. Both inhibit fungal and bacterial xylanases, and their modes of action differ depending on the isoform and the target enzyme [17].

Among the numerous plant protein inhibitors of glycoside hydrolases identified so far, the polygalacturonase-inhibiting proteins are the only ones showing a strict preference for fungal enzymes [36–38]. Whereas the structures of fungal polygalacturonases are conserved [37], the fungal xylanases show distinctive structural differences between families 10 and 11 [13,14]. In addition, the mechanism of inhibition of the polygalacturonase-inhibiting proteins towards fungal polygalacturonases varies depending on the source, e.g. the major isoform from pear fruit is a competitive inhibitor of several fungal polygalacturonases [39], whereas that from raspberry fruit [40] and bean hypocotyls [41] inhibited via a non-competitive mechanism.

In conclusion, we present a detailed mechanistic study on the inhibition of fungal xylanases by the proteinaceous xylanase inhibitor XIP-I from wheat. This is the first mechanistic study of any xylanase inhibitor.

This work was supported by grants from the Biotechnology and Biological Sciences Research Council and from the European Commission (GEMINI QLK1-2000-00811). J.E.L. is supported by a Welcome Trust Senior Research Fellowship. We thank Dr Maija Tankanen, Professors Jan Delcour, Anthony Clarke, Gideon Davis, Harry Gilbert and Francisco J. Pastor for providing xylanase enzymes. We also thank Dr Fred Mellon for MS analysis, and Dr Alain Roussel for help in calculation of the surface area of proteins.

REFERENCES

1 Jaynes, T. A. and Nelson, O. E. (1970) An invertase inactivator in maize endosperms and factors affecting inactivation. Plant Physiol. **47**, 629–634
2 Pressey, R. (1993) Invertase inhibitor in tomato fruit. Phytochemistry **36**, 543–546
3 Greiner, S., Krausgrill, S. and Rausch, T. (1998) Cloning of a tobacco apoplasmic invertase inhibitor. Proof of function of the recombinant protein and expression analysis during plant development. Plant Physiol. **116**, 733–742
4 Macri, L. J., Macgregor, A. W., Schroeder, S. W. and Bazin, S. L. (1993) Detection of a limit dextrinase inhibitor in barley. J. Cer. Sci. **18**, 103–106
5 Albersheim, P. and Anderson, A. J. (1971) Proteins from plant cell walls inhibit polygalacturonases secreted by plant pathogens. Proc. Natl. Acad. Sci. U.S.A. **68**, 1815–1819
6 Stotz, H. U., Contos, J. A., Powell, A. T., Bennett, A. B. and Labavitch, J. M. (1994) Structure and expression of an inhibitor of fungal polygalacturonases from tomato. Plant Mol. Biol. **25**, 607–617
7 Giovane, A., Balestrieri, C., Quagliuolo, L., Castaldo, D. and Servillo, L. (1995) A glycoprotein inhibitor of pectin methylesterase in kiwi fruit – purification by affinity-chromatography and evidence of a ripening-related precursor. Eur. J. Biochem. **233**, 926–929
8 Weselake, R. J., Macgregor, A. W. and Hill, R. D. (1983) An endogenous α-amylase inhibitor in barley kernels. Plant Physiol. **72**, 809–812
9 Le Berre Anton, V., Bompard Gilles, C., Payan, F. and Rouge, P. (1997) Characterization and functional properties of the α-amylase inhibitor (α-AI) from kidney bean (*Phaseolus vulgaris*) seeds. Biochim. Biophys. Acta **1343**, 31–40
10 Debyser, W., Derdelinckx, G. and Delcour, J. A. (1997) Arabinoxylan solubilization and inhibition of the barley malt xylanolytic system by wheat during mashing with wheat wholemeal adjunct: evidence for a new class of enzyme inhibitors in wheat. J. Am. Soc. Brew. Chem. **55**, 153–156
11 Rouau, X. and Surget, A. (1998) Evidence for the presence of a pentosanase inhibitor in wheat flours. J. Cer. Sci. **28**, 63–70
12 Debyser, W., Peumans, W. J., Van Damme, E. M. and Delcour, J. A. (1999) *Triticum aestivum* xylanase inhibitor (TAXI), a new class of enzyme inhibitor affecting breadmaking performance. J. Cer. Sci. **30**, 39–43
13 Henrissat, B. (1991) A classification of glycosyl hydrolases based on amino acid sequence similarities. Biochem. J. **280**, 309–316
14 Davies, G. and Henrissat, B. (1995) Structures and mechanisms of glycosyl hydrolases. Structure **3**, 853–859
15 Kulkarni, N., Shendye, A. and Rao, M. (1999) Molecular and biotechnological aspects of xylanases. FEMS Microbiol. Rev. **23**, 411–456
16 McLauchlan, W. R., Garcia-Conesa, M. T., Williamson, G., Roza, M., Ravestein, P. and Maat, J. (1999) A novel class of protein from wheat which inhibits xylanases. Biochem. J. **338**, 441–446
17 Gebruers, K., Debyser, W., Goesaert, H., Proost, P., Van Damme, J. and Delcour, J. A. (2001) *Triticum aestivum* L. endoxylanase inhibitor (TAXI) consists of two inhibitors, TAXI I and TAXI II, with different specificities. Biochem. J. **353**, 239–244
18 Berrin, J. G., Williamson, G., Puigserver, A., Chaix, J. C., McLauchlan, W. R. and Juge, N. (2000) High-level production of recombinant fungal endo-β-1,4-xylanase in the methylotrophic yeast *Pichia pastoris*. Protein Expr. Purif. **19**, 179–187
19 MacCabe, A. P., Fernandez-Espinar, M. T., de Graaff, L. H., Visser, J. and Ramon, D. (1996) Identification, isolation and sequence of the *Aspergillus nidulans xlnC* gene encoding the 34-kDa xylanase. Gene **175**, 29–33
20 Bradford, M. M. (1976) A rapid and sensitive method for the quantitation of microgram quantities of protein utilizing the principle of protein–dye binding. Anal. Biochem. **72**, 248–254
21 Bailey, M. J., Biely, P. and Poutanen, K. (1992) Interlaboratory testing of methods for assay of xylanase activity. J. Biotechnol. **23**, 257–270
22 Johnsson, B., Lofas, S. and Lindquist, G. (1991) Immobilization of proteins to a carboxymethyldextran-modified gold surface for biospecific interaction analysis in surface plasmon resonance sensors. Anal. Biochem. **198**, 268–277
23 Jonsson, U., Fagerstam, L., Ivarsson, B., Johnsson, B., Karlsson, R., Lundh, K., Lofas, S., Persson, B., Roos, H. and Ronnberg, I. (1991) Real-time biospecific interaction analysis using surface plasmon resonance and a sensor chip technology. Biotechniques **11**, 620–627
24 Wiseman, T., Williston, S., Brandts, J. F. and Lin, L. N. (1989) Rapid measurement of binding constants and heats of binding using a new titration calorimeter. Anal. Biochem. **179**, 131–137
25 Lin, Z., Schwartz, F. P. and Eisenstein, E. (1995) The hydrophobic nature of GroEL-substrate binding. J. Biol. Chem. **270**, 1011–1014
26 Ladbury, J. E., Wright, J. G., Sturtevant, J. M. and Sigler, P. B. (1994) A thermodynamic study of the trp repressor–operator interaction. J. Mol. Biol. **238**, 669–681

27 Livingstone, J. R., Spolar, R. S. and Record, Jr, M. T. (1991) Contribution to the thermodynamics of protein folding from the reduction in water-accessible nonpolar surface area. Biochemistry **30**, 4237–4244
28 Spolar, R. S. and Record, Jr, M. T. (1994) Coupling of local folding to site-specific binding of proteins to DNA. Science **263**, 777–784
29 Wilcox, E. R. and Whitaker, J. R. (1984) Some aspects of the mechanism of complexation of red kidney bean α-amylase inhibitor and α-amylase. Biochemistry **23**, 1783–1791
30 Morrison, J. F. and Walsh, C. T. (1988) The behavior and significance of slow-binding enzyme inhibitors. Adv. Enzymol. Relat. Areas Mol. Biol. **61**, 201–301
31 Legler, G. (1990) Glycoside hydrolases: mechanistic information from studies with reversible and irreversible inhibitors. Adv. Carbohydr. Chem. Biochem. **48**, 319–384
32 Koukiekolo, R., Le Berre Anton, V., Desseaux, V., Moreau, Y., Rouge, P., Marchis Mouren, G. and Santimone, M. (1999) Some aspects of the mechanism of complexation of red kidney bean α-amylase inhibitor and α-amylase. Eur. J. Biochem. **265**, 20–26
33 Weselake, R. J., Macgregor, A. W., Hill, R. D. and Duckworth, H. W. (1983) Purification and characteristics of an endogenous α-amylase inhibitor from barley kernels. Plant Physiol. **73**, 1008–1012
34 Lo Conte, L., Chothia, C. and Janin, J. (1999) The atomic structure of protein–protein recognition sites. J. Mol. Biol. **285**, 2177–2198
35 Bompard Gilles, C., Rousseau, P., Rouge, P. and Payan, F. (1996) Substrate mimicry in the active center of a mammalian α-amylase: structural analysis of an enzyme–inhibitor complex. Structure **4**, 1441–1452
36 Collmer, A. and Keen, N. T. (1986) The role of pectic enzymes in plant pathogenesis. Annu. Rev. Phytopathol. **24**, 383–409
37 Cervone, F., De Lorenzo, G., Pressey, R., Darvill, A. G. and Albersheim, P. (1990) Host pathogen interactions .35. Can *Phaseolus* PGIP inhibit pectic enzymes from microbes and plants? Phytochemistry **29**, 447–449
38 Bergmann, C. W., Ito, Y., Singer, D., Albersheim, P., Darvill, A. G., Benhamou, N., Nuss, L., Salvi, G., Cervone, F. and De Lorenzo, G. (1994) Polygalacturonase-inhibiting protein accumulates in *Phaseolus vulgaris* in response to wounding, elicitors and fungal infection. Plant J. **5**, 625–634
39 Abugoukh, A. A., Strand, L. L. and Labavitch, J. M. (1983) Development-related changes in decay susceptibility and polygalacturonase inhibitor content of Bartlett pear fruit. Physiol. Plant Pathol. **23**, 101–109
40 Johnston, D. J., Ramanathan, V. and Williamson, B. (1993) A protein from immature raspberry fruits which inhibits endopolygalacturonases from *Botrytis cinerea* and other micro-organisms. J. Exp. Bot. **44**, 971–976
41 Lafitte, C., Barthe, J. P., Montillet, J. L. and Touze, A. (1984) Glycoprotein inhibitors of *Colletotrichum lindemuthianum* endopolygalacturonase in near isogenic lines of *Phaseolus vulgaris* resistant and susceptible to anthracnose. Physiol. Plant Pathol. **25**, 39–53

Received 28 January 2002/26 March 2002; accepted 16 April 2002
Published as BJ Immediate Publication 16 April 2002, DOI 10.1042/BJ20020168